JCTC Journal of Chemical Theory and Computation

Theoretical Study on the Structure and the Frequency of Isomers of the Naphthalene Dimer

Morihisa Saeki* and Hiroshi Akagi

Quantum Beam Science Directorate, Japan Atomic Energy Agency, Tokai-mura, Naka-gun, Ibaraki 319-1195, Japan

Masaaki Fujii

Chemical Resources Laboratory, Tokyo Institute of Technology, 4259 Nagatsuta-cho, Midori-ku, Yokohama 226-8503, Japan

Received November 11, 2005

Abstract: The structures of the naphthalene monomer and dimer were investigated with performing vibrational analysis. The MP2 optimization showed that the naphthalene monomer has a nonplanar geometry in the 6-31G, 6-31G*, 6-31+G*, and 6-311G basis sets, while it has a planar geometry in the 6-31G*(0.25) and Dunning's correlation consistent basis sets. The MP2/cc-pVDZ calculation showed the presence of the four stable isomers, which were part of the isomers in the previous MP2/6-31G* calculation (Walsh, T. R. *Chem. Phys. Lett.* **2002**, *363*, 45). The presence of extra structures in the MP2/6-31G* calculation is attributed to a poor description of the potential energy surface, which is evident from the nonplanar structure of the monomer in the MP2/6-31G* calculation. The relative stability among the isomers in the MP2/cc-pVDZ calculation without counterpoise correction was maintained in both the single-point calculation at the MP2/aug-cc-pVDZ//MP2/cc-pVDZ level and the counterpoise-corrected optimization at the MP2/cc-pVDZ level. The relative stability among the isomers suggested an enhancement of the $\pi-\pi$ interaction in the structure with lower symmetry, which could be explained using a molecular-orbital model. The vibrational analysis in MP2/cc-pVDZ without the counterpoise correction suggested that the isomers of the naphthalene dimer were distinguishable by the observation of the infrared spectrum in the low-frequency region (150−600 cm^{-1}).

Introduction

Intermolecular interactions between polycyclic aromatic hydrocarbon (PAH) molecules are unique, because the π-type molecular orbitals contribute them. The π orbital of one PAH molecule interacts with the π orbital or the C−H bonding of the other. The interaction with the π orbital is called a $\pi-\pi$ interaction (also called a stacking interaction), while that with the C−H bonding is named a C−H$\cdots\pi$ interaction. The relative strength between these interactions determines the structure of PAH clusters.

Much concerted effort between experiment and theory was made to study several dimers of PAH:benzene,[1−14] naphthalene,[1−3,15−21] and anthracene[22,23] dimers. Especially, the structure of the benzene dimer has allured controversies for a long time. Klemperer et al. have suggested a structure dominated by the C−H$\cdots\pi$ interaction (T-shaped structure) using molecular beam electronic resonance spectroscopy.[5] Bernstein et al., however, have claimed that the structure dominated by the $\pi-\pi$ interaction (sandwich structure) may be more stable than the T-shaped structure based on their theoretical consideration.[7] A final conclusion has been given by Felker et al.[8−11] They observed the splitting of the vibrational band in the Raman spectrum, which was attributed

* Corresponding author phone: +81-29-282-6100; e-mail: saeki.morihisa@jaea.go.jp.

10.1021/ct050278n CCC: $33.50
Published on Web 05/17/2006

Table 1. Basis-Set Dependence of Symmetry, Energy (hartree), and C−C Bond Length (Å) of Naphthalene Monomer

			bond length[b]			
	symmetry	energy	C1−C2	C2−C3	C5−C10	C1−C10
6-31G	C_{2h}	−384.08453	1.393 (+0.022)	1.432 (+0.020)	1.446 (+0.026)	1.436 (+0.014)
6-31G*	C_{2h}	−384.61466	1.379 (+0.008)	1.415 (+0.003)	1.432 (+0.012)	1.419 (−0.003)
6-31+G*	C_{2h}	−384.63770	1.382 (+0.011)	1.416 (+0.004)	1.433 (+0.013)	1.421 (−0.001)
6-311G	C_{2h}	−384.20668	1.388 (+0.017)	1.428 (+0.016)	1.441 (+0.021)	1.432 (+0.010)
6-31G*(0.25)	D_{2h}	−384.36700	1.402 (+0.031)	1.438 (+0.026)	1.456 (+0.036)	1.440 (+0.018)
cc-pVDZ	D_{2h}	−384.68161	1.389 (+0.018)	1.423 (+0.011)	1.441 (+0.021)	1.427 (+0.005)
aug-cc-pVDZ	D_{2h}	−384.73937	1.392 (+0.021)	1.425 (+0.013)	1.444 (+0.024)	1.428 (+0.006)
cc-pVTZ	D_{2h}	−385.04465	1.377 (+0.006)	1.411 (−0.001)	1.430 (+0.010)	1.415 (−0.007)
exptl[a]			1.371	1.412	1.420	1.422

[a] Experimetal bond length is obtained from ref 30. [b] The value in the parentheses indicates the difference between the calculated and experimental bond length.

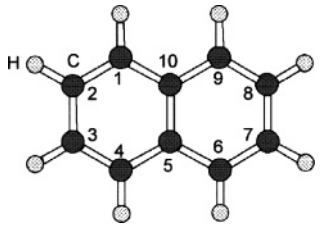

Figure 1. Definition of the label of the naphthalene monomer.

to a structure dominated by the C−H···π interaction. A measurement of the depolarization ratio of the Raman band by Ebata et al. has supported the conclusion given by Felker et al.[12] The discrepancy between the experiment and the calculation indicates the difficulty to accurately calculate the $\pi-\pi$ and C−H···π interactions.

The information concerning the structure of the naphthalene dimer is not rich compared with that of the benzene dimer. Saigusa et al. have investigated the electronic structure of the naphthalene dimer using a resonant two-photon ionization (R2PI).[15,16] The electronic spectrum was shown to be broad and structureless. Considering that sharp bands were observed in the spectrum of the benzene dimer,[4] the structure of the naphthalene dimer is assumed to be different from that of the benzene dimer. There have been many theoretical studies about the structure of the naphthalene dimer.[1−3,17−21] These studies suggest that the $\pi-\pi$ interaction was adequately estimated by a calculation including the electron correlation, diffuse orbital, and the basis set superposition error (BSSE) correction. However, considerations of both the electron correlation and the diffuse orbital burden the calculation of the naphthalene dimer, because it is a large system containing 20 carbon atoms and 16 hydrogen atoms. Gonzalez and Lim expressed the dilemma as follows:[1] "Unfortunately, because of the large size of these species (*benzene, naphthalene and anthracene dimer*), the basis sets that can be employed to obtain conformational geometries and energies from ab initio calculations are rather limited in size. Moreover, because dispersion effects are important in determining the geometries of vdW dimer, SCF calculations are completely inadequate and methodologies that include electron correlation must be employed". Concerning the dilemma, most researchers have not calculated the frequencies of the naphthalene dimer, although vibrational analysis is essential to ensure that the optimized structures are located in the local minimum.

Recently Walsh has optimized the geometry of the naphthalene dimer while calculating the frequencies at MP2/6-31G* level.[20] He found a new structure of naphthalene dimer belonging to the C_2 point group, which was the most stable among the isomers. However, as described in this paper, the naphthalene monomer has a nonplanar geometry in the MP2/6-31G* calculation. For assurance of the stability of the new structure, the isomers of the naphthalene dimer should be investigated using the computational level whose monomer is calculated to be planar. First, we optimized the structure of the monomer using various basis sets and determined the computational level adequate for the calculation of naphthalene. At the determined level, the isomers of naphthalene dimer were investigated with performing the vibrational analysis. The relative stability among the obtained isomers was explained using a molecular-orbital model. Based on the result of the vibrational analysis of the monomer and the dimer, we discussed the vibrational modes available to experimentally distinguish the isomers.

Computational Method

The used program was the GAUSSIAN 98[24] and the GAUSSIAN 03 package.[25] Optimizations of the naphthalene monomer and dimer were carried out by the MP2 method with the frozen core approximation, because the electron correlation must be considered for precisely estimating the $\pi-\pi$ interaction.[1−3,18−21,26] The initial structure of the dimer employed in this study is the same as that in Walsh's work.[20] The stability of the optimized structures was checked by a harmonic frequency analysis. The frequency was computed analytically. If the optimized structure had one or more imaginary frequencies with fixed symmetry, it was reoptimized with the lower symmetry. The procedure was iterated until the true local minimum structure was obtained. In estimating the binding energy of the dimer, BSSE was corrected using the counterpoise (CP) method.[27] In addition to these procedures, we optimized the geometry of the

naphthalene dimer with considering the CP correction. The geometrical optimization with CP was performed using "Counterpoise" keyword in GAUSSIAN 03. This keyword runs the optimization process developed by Simon et al.[28] All of the computations were carried out on an NEC SX-7 computer at Research Center for Computational Science, Okazaki, Japan.

Results

Basis-Set Dependence of the Structure of the Naphthalene Monomer. The structure of the naphthalene monomer was optimized with 6-31G, 6-31G*, 6-31+G*, 6-311G, 6-31G*-(0.25), cc-pVDZ, aug-cc-pVDZ, and cc-pVTZ basis sets. The 6-31G*(0.25) basis set is 6-31G* with the exponent on the d function reduced to 0.25 (0.80 in the 6-31G*) and was developed to describe the $\pi-\pi$ interaction.[26,29] The calculated symmetry, energy, and bond length of naphthalene are listed in Table 1, together with the experimental bond length in ref 30. The label of the carbon atom used for the geometrical parameter is defined in Figure 1. The optimized geometry belongs to the C_{2h} point group in the MP2/6-31G calculation, although it should belong to the D_{2h} point group. This means that the naphthalene molecule is distorted out of the plane. The distortion is kept in calculations with the 6-31G*, 6-31+G*, 6-311G basis sets, while the naphthalene monomer has the planar geometry in 6-31G*(0.25), cc-pVDZ, aug-cc-pVDZ, and cc-pVTZ. The results suggested that a correct calculation of naphthalene is accomplished by the 6-31G*-(0.25) and Dunning's correlation consistent basis sets at the MP2 level. The comparison between the calculation and the experiment suggests that the calculated bond lengths are drastically improved from MP2/6-31G*(0.25) to MP2/cc-pVDZ. The bond lengths in MP2/aug-cc-pVDZ show a worse agreement with the experimental values than those in MP2/cc-pVDZ. It means that the structure of the monomer cannot be refined by the addition of the diffuse functions to the cc-pVDZ. On the other hand, there is very good agreement of the bond lengths between the MP2/cc-pVTZ calculation and the experiment. The agreement with the experiment becomes better with the ordering of 6-31G*(0.25) < aug-cc-pVDZ < cc-pVDZ < cc-pVTZ. The MP2/cc-pVTZ level is most adequate for the calculation of naphthalene but consumes computational resources very much. Thus, we selected the MP2/cc-pVDZ level for the calculation of the naphthalene dimer.

Frequency of the Naphthalene Monomer in MP2/cc-pVDZ. The naphthalene molecule has 48 normal modes, whose symmetries are $9a_{1g}+8b_{3g}+3b_{1g}+4b_{2g}+4a_{1u}+4b_{3u}+8b_{1u}+8b_{2u}$. The frequencies in the MP2/cc-pVDZ calculation are listed in Table 2. The types of the vibrational modes are noted as *r*(CH) for CH stretching, *R*(CC) for CC stretching, β(CH) for CH in-plane bending, α(CCC) for CCC in-plane bending, ϵ(CH) for CH out-of-plane bending, and τ(CCC) for CCC out-of-plane bending vibration. The assignment of the vibrational types follows Ellinger's work.[31] The experimental frequencies were obtained from ref 32.

The scaling factor is populated between 0.9 and 1.1 in all modes, except for the ν_{23} mode ($\sim$1.5). The extraordinary value in the ν_{23} mode may be attributed to an incorrect assignment, because the calculated frequencies of other modes have good agreement with the experimental ones. The

Table 2. Calculated and Experimental Frequency (cm^{-1}) of the Vibrational Modes of the Naphthalene Monomer

mode	symmetry	frequency: calcd	frequency: exptl[b]	scaling factor[d]
		r(CH) Type[a]		
ν_1	a_{1g}	3239	3060	0.9447
ν_2	a_{1g}	3209	3031	0.9445
ν_{10}	b_{3g}	3224	3092	0.9591
ν_{11}	b_{3g}	3203	3060	0.9554
ν_{33}	b_{1u}	3225	3065	0.9504
ν_{34}	b_{1u}	3204	3058	0.9544
ν_{41}	b_{2u}	3238	3090	0.9543
ν_{42}	b_{2u}	3207	3027	0.9439
		averaged scaling factor		0.9508 (0.0059)
		β(CH) Type[a]		
ν_6	a_{1g}	1170	1145	0.9786
ν_{15}	b_{3g}	1161	1158	0.9974
ν_{36}	b_{1u}	1406	1389	0.9879
		averaged scaling factor		0.9880 (0.0094)
		α(CCC) Type[a]		
ν_9	a_{1g}	514	512	0.9961
ν_{16}	b_{3g}	931	936	1.0054
ν_{17}	b_{3g}	506	506	1.0000
ν_{39}	b_{1u}	803	747	0.9303
ν_{40}	b_{1u}	356	359	1.0084
ν_{48}	b_{2u}	618	618	1.0000
		averaged scaling factor		0.9900 (0.0296)
		R(CC) + β(CH) Type[a]		
ν_4	a_{1g}	1490	1460	0.9799
ν_7	a_{1g}	1051	1025	0.9753
ν_{44}	b_{2u}	1495	1361	0.9104
ν_{45}	b_{2u}	1255	1209	0.9633
ν_{46}	b_{2u}	1170	1138	0.9726
		averaged scaling factor		0.9603 (0.0285)
		R(CC) + β(CH) + α(CCC) Type[a]		
ν_3	a_{1g}	1625	1577	0.9705
ν_5	a_{1g}	1458	1376	0.9438
ν_8	a_{1g}	771	758	0.9831
ν_{12}	b_{3g}	1688	1624	0.9621
ν_{13}	b_{3g}	1484	1438	0.9690
ν_{14}	b_{3g}	1255	1239	0.9873
ν_{35}	b_{1u}	1637	1595	0.9743
ν_{37}	b_{1u}	1277	1265	0.9906
ν_{38}	b_{1u}	1139	1125	0.9877
ν_{43}	b_{2u}	1562	1509	0.9661
ν_{47}	b_{2u}	1042	1008	0.9674
		averaged scaling factor		0.9729 (0.0138)
		ϵ(CH) Type[a]		
ν_{18}	b_{1g}	924	943	1.0206
ν_{19}	b_{1g}	721	717	0.9945
ν_{21}	b_{2g}	951	980	1.0305
ν_{22}	b_{2g}	849	876	1.0318
ν_{25}	a_{1u}	933	970	1.0397
ν_{26}	a_{1u}	837	841	1.0048
ν_{29}	b_{3u}	932	958	1.0279
ν_{30}	b_{3u}	785	782	0.9962
		averaged scaling factor		1.0182 (0.0174)
		τ(CCC) Type[a]		
ν_{20}	b_{1g}	377	386	1.0239
ν_{23}	b_{2g}	535	846	1.5813
ν_{24}	b_{2g}	451	461	1.0222
ν_{27}	a_{1u}	558	581	1.0412
ν_{28}	a_{1u}	182	195	1.0714
ν_{31}	b_{3u}	463	476	1.0281
ν_{32}	b_{3u}	168	176	1.0476
		averaged scaling factor		1.0391 (0.0187)[c]

[a] The type of the vibrational modes are noted as *r*(CH) for CH stretching, *R*(CC) for CC stretching, β(CH) for CH in-plane bending, α(CCC) for CCC in-plane bending, ϵ(CH) for CH out-of-plane bending, and τ(CCC) for CCC out-of-plane bending vibration. [b] Experimetal value is obtained from ref 32. [c] The ν_{23} mode is neglected in averaging of the scaling factor. [d] Averaged scaling factors are calculated in the respective type. The value in the parentheses indicates standard deviation.

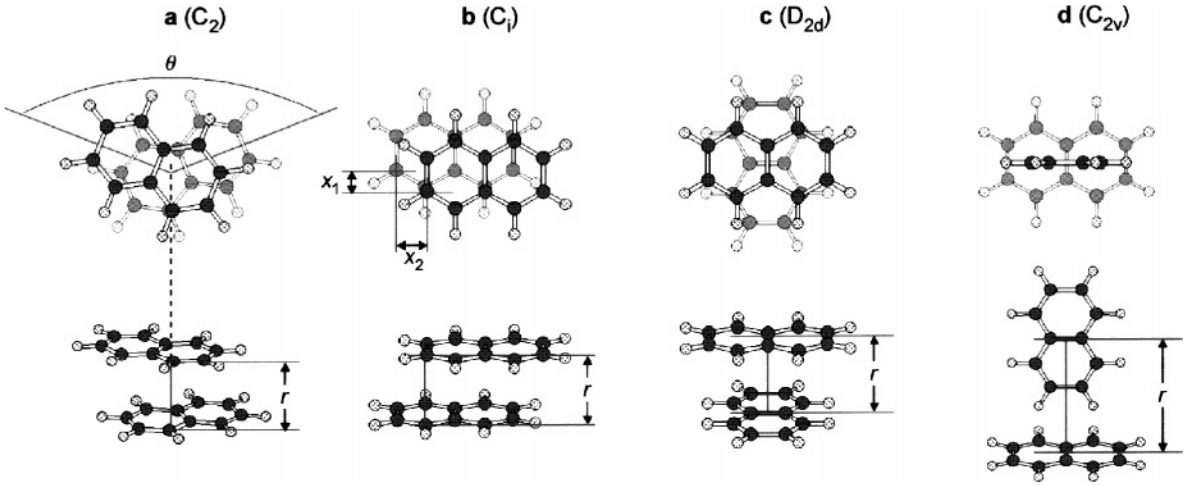

Figure 2. Optimized isomers of the naphthalene dimer in the MP2/cc-pVDZ calculation. The symbol in the parenthesis indicates the symmetry of each structure. The geometries and energies of these structures are summarized in Table 3.

Table 3. Dependence of Geometry and Binding Energy D_0 (kcal/mol) on Computational Method in Structures **a**−**d**[a]

	a			**b**				**c**		**d**	
method	r	θ	D_0	r	x_1	x_2	D_0	r	D_0	r	D_0
Geometry without CP											
MP2/cc-pVDZ	3.24	136	−5.30	3.20	0.93	1.25	−5.00	3.25	−4.53	5.86	−3.55
MP2/aug-cc-pVDZ//MP2/cc-pVDZ			−10.95				−10.34		−9.48		−5.68
Geometry with CP											
MP2/cc-pVDZ	3.46	135	−6.24	3.40	1.03	1.31	−5.89	3.48	−5.38	6.03	−3.80

[a] The unit of the geometrical parameters is degree in θ and angstrom in r, x_1, and x_2. The geometry of the naphthalene dimer was optimized without and with the CP correction in MP2/cc-pVDZ. Single-point calculation at the MP2/aug-cc-pVDZ level was performed using the optimized geometry in MP2/cc-pVDZ without CP. All binding energies are CP corrected.

modes of the r(CH), β(CH), α(CCC), R(CC)+β(CH), and R(CC)+β(CH)+α(CCC) types are in-plane vibration, while those of the ϵ(CH) and τ(CCC) types are out-of-plane vibration. The averaged scaling factor suggests that the calculated frequency is overestimated in the in-plane vibrations and is underestimated in the out-of-plane ones. The overestimation of the frequency of the out-of-plane vibrations has been found in the calculation of benzene.[33,34] In the harmonic frequency analysis the calculated frequency should be overestimated, because the anharmonicity is neglected. The underestimation in the out-of-plane vibration indicates a poor description of the potential surface along the out-of-plane direction.

Stable Isomers of the Naphthalene Dimer. Figure 2 shows stable structures of the naphthalene dimer in the MP2/cc-pVDZ calculation. The geometries and energies of structures **a**−**d** are summarized in Table 3. Walsh has suggested eight isomers were stable in the MP2/6-31G* calculation.[20] However, the MP2/cc-pVDZ calculation elucidated that structures **a**−**d** were located in the local minimum, while the others were in transition states. We compared the calculated geometry of the naphthalene molecules between the monomer and the dimer and found that the geometrical parameters in the monomer are almost maintained in the dimer. The naphthalene molecules are bound by the $\pi-\pi$ interaction in structures **a**−**c** and by the C−H···π interaction in structure **d**. The counterpoise-corrected binding energy is 4.5−5.3 kcal/mol in structures **a**−**c**, while it is 3.6 kcal/mol in structure **d**. The binding energy ordering is **a** > **b** > **c** > **d**. Structure **a**, which corresponds to the isomer newly found by Walsh,[20] is most stable among structures **a**−**d**. There is little difference of the intermolecular distance r among structures **a**−**c**.

To investigate the basis-set dependence of the relative stability among the isomers, we performed the single-point calculation at the MP2/aug-cc-pVDZ level using the optimized geometry in MP2/cc-pVDZ. As shown in Table 3, the ordering of the CP-corrected binding energy in the MP2/cc-pVDZ calculation is kept in MP2/aug-cc-pVDZ//MP2/cc-pVDZ. The binding energy in structures **a**−**c** increases by 5.0−5.7 kcal/mol from MP2/cc-pVDZ to MP2/aug-cc-pVDZ, while that in structure **d** increases by only 2.1 kcal/mol. It indicates that the addition of diffuse functions has a larger effect on the $\pi-\pi$ interaction than on the C−H···π interaction.

In clusters the optimization with the CP correction may refine the geometry optimized without CP, because the estimation of the intermolecular interaction is improved.[28] Using the obtained isomers in MP2/cc-pVDZ without CP as the initial geometry, we investigated the geometrical change with the CP correction. As shown in Table 3, the intermolecular distance r was elongated by ∼0.2 Å in every structure when the CP correction was considered. In principle, since the BSSE causes the intermolecular interactions to be artificially too attractive, the CP correction should make the cluster less stable.[28] Consequently, the intermolecular distance will be longer when the cluster is optimized with the CP correction. The ordering of the binding energy is the same between geometry with CP and without CP. The binding energy of the geometry with CP is larger than that

Table 4. Calculated Frequency (cm^{-1}) of the Intramolecular Vibrational Modes of the Naphthalene Dimer in the MP2/cc-pVDZ Calculation without CP[a]

mode	a	b	c	d	mode	a	b	c	d
				r(CH) Type (Scaling Factor 0.9508)					
	3077(b)	3079(a_u)	3074(a_1)	3095(a_1)		3077(a)	3079(a_g)	3074(b_2)	3084(b_2)
	3073(b)	3074(a_u)	3073(e)	3079(a_1)		3073(a)	3074(a_g)	3073(e)	3078(b_2)
	3063(a)	3063(a_u)	3062(e)	3077(a_1)		3062(b)	3063(a_g)	3062(e)	3066(b_1)
	3060(a)	3061(a_g)	3062(b_1)	3066(a_2)		3060(b)	3061(a_u)	3061(a_2)	3064(b_2)
	3052(a)	3048(a_g)	3050(b_2)	3052(a_1)		3051(b)	3047(a_u)	3049(a_1)	3050(b_2)
	3044(b)	3046(a_u)	3048(e)	3049(a_1)		3044(a)	3046(a_g)	3048(e)	3048(b_1)
	3043(a)	3042(a_u)	3043(e)	3047(a_2)		3042(b)	3041(a_g)	3043(e)	3046(a_1)
	3039(a)	3040(a_g)	3043(a_2)	3045(b_2)		3039(b)	3040(a_u)	3042(b_1)	3043(b_2)
				β(CH) Type (Scaling Factor 0.9880)					
ν_6^+	1154(b)	1155(a_u)	1153(a_1)	1160(a_1)	ν_6^-	1152(a)	1154(a_g)	1152(b_2)	1155(a_1)
ν_{15}^+	1143(b)	1144(a_g)	1145(b_1)	1149(b_2)	ν_{15}^-	1143(a)	1143(a_u)	1143(a_2)	1146(a_2)
ν_{36}^+	1387(a)	1387(a_u)	1387(e)	1389(b_2)	ν_{36}^-	1387(b)	1387(a_g)	1387(e)	1389(b_1)
				α(CCC) Type (Scaling Factor 0.9900)					
ν_9^+	508(a)	509(a_g)	509(b_2)	511(a_1)	ν_9^-	508(b)	508(a_u)	508(a_1)	509(a_1)
ν_{16}^+	921(a)	920(a_g)	920(a_2)	920(b_2)	ν_{16}^-	919(b)	920(a_u)	920(b_1)	919(a_2)
ν_{17}^+	499(a)	503(a_u)	499(b_1)	502(b_2)	ν_{17}^-	499(b)	500(a_g)	499(a_2)	501(a_2)
ν_{39}^+	794(b)	794(a_u)	794(e)	795(b_1)	ν_{39}^-	793(a)	793(a_g)	794(e)	795(b_2)
ν_{40}^+	351(a)	351(a_u)	351(e)	353(b_2)	ν_{40}^-	351(b)	351(a_g)	351(e)	352(b_1)
ν_{48}^+	610(b)	610(a_u)	610(e)	612(a_1)	ν_{48}^-	609(a)	610(a_g)	610(e)	611(b_2)
				R(CC)+β(CH) Type (Scaling Factor 0.9603)					
ν_4^+	1430(b)	1431(a_u)	1431(a_1)	1431(a_1)	ν_4^-	1429(a)	1430(a_g)	1430(b_2)	1430(a_1)
ν_7^+	1009(a)	1008(a_g)	1009(b_2)	1008(a_1)	ν_7^-	1008(b)	1008(a_u)	1008(a_1)	1008(a_1)
ν_{44}^+	1453(b)	1451(a_g)	1449(e)	1439(b_2)	ν_{44}^-	1451(a)	1450(a_u)	1449(e)	1438(a_1)
ν_{45}^+	1205(a)	1206(a_u)	1206(e)	1206(a_1)	ν_{45}^-	1205(b)	1205(a_g)	1206(e)	1206(b_2)
ν_{46}^+	1122(a)	1121(a_g)	1122(e)	1124(b_2)	ν_{46}^-	1122(b)	1120(a_u)	1122(e)	1123(a_1)
				R(CC)+β(CH)+α(CCC) Type (Scaling Factor 0.9729)					
ν_3^+	1576(b)	1577(a_g)	1575(b_2)	1579(a_1)	ν_3^-	1574(a)	1575(a_u)	1575(a_1)	1578(a_1)
ν_5^+	1420(b)	1420(a_u)	1420(a_1)	1419(a_1)	ν_5^-	1420(a)	1419(a_g)	1419(b_2)	1418(a_1)
ν_8^+	750(a)	749(a_g)	750(a_1)	750(a_1)	ν_8^-	749(b)	749(a_u)	749(b_2)	749(a_1)
ν_{12}^+	1638(b)	1638(a_g)	1638(a_2)	1641(b_2)	ν_{12}^-	1638(a)	1638(a_u)	1638(b_1)	1640(a_2)
ν_{13}^+	1440(a)	1441(a_g)	1442(b_1)	1442(a_2)	ν_{13}^-	1440(b)	1441(a_u)	1441(a_2)	1442(b_2)
ν_{14}^+	1217(a)	1218(a_g)	1218(b_1)	1221(a_2)	ν_{14}^-	1217(b)	1218(a_u)	1218(a_2)	1219(b_2)
ν_{35}^+	1587(a)	1588(a_u)	1589(e)	1591(b_2)	ν_{35}^-	1586(b)	1587(a_g)	1589(e)	1590(b_1)
ν_{37}^+	1240(a)	1240(a_u)	1241(e)	1243(b_1)	ν_{37}^-	1240(b)	1240(a_g)	1241(e)	1241(b_2)
ν_{38}^+	1105(b)	1105(a_u)	1105(e)	1109(b_2)	ν_{38}^-	1104(a)	1105(a_g)	1105(e)	1107(b_1)
ν_{43}^+	1518(b)	1518(a_g)	1517(e)	1518(a_1)	ν_{43}^-	1518(a)	1518(a_u)	1517(e)	1517(b_2)
ν_{47}^+	1014(b)	1014(a_u)	1013(e)	1013(b_2)	ν_{47}^-	1013(a)	1013(a_g)	1013(e)	1013(a_1)
				ϵ(CH) Type (Scaling Factor 1.0182)					
ν_{18}^+	926(a)	928(a_u)	927(e)	940(b_2)	ν_{18}^-	925(b)	927(a_g)	927(e)	940(b_1)
ν_{19}^+	728(b)	730(a_u)	727(e)	736(b_1)	ν_{19}^-	726(a)	725(a_g)	727(e)	735(b_2)
ν_{21}^+	957(b)	957(a_u)	955(e)	967(b_1)	ν_{21}^-	955(a)	955(a_g)	955(e)	965(a_2)
ν_{22}^+	856(a)	858(a_u)	854(e)	866(b_1)	ν_{22}^-	852(b)	853(a_g)	854(e)	865(a_2)
ν_{25}^+	938(a)	938(a_g)	937(a_2)	948(a_2)	ν_{25}^-	936(b)	936(a_u)	934(b_1)	945(a_2)
ν_{26}^+	842(a)	845(a_g)	845(b_1)	853(a_2)	ν_{26}^-	840(b)	843(a_u)	839(a_2)	852(a_2)
ν_{29}^+	933(b)	936(a_g)	937(b_2)	947(a_1)	ν_{29}^-	933(a)	933(a_u)	934(a_1)	947(b_1)
ν_{30}^+	789(a)	792(a_g)	795(a_1)	800(b_1)	ν_{30}^-	787(b)	788(a_u)	788(b_2)	799(a_1)
				τ(CCC) Type (Scaling Factor 1.0391)					
ν_{20}^+	387(b)	387(a_u)	387(e)	393(b_1)	ν_{20}^-	386(a)	385(a_g)	387(e)	388(b_2)
ν_{23}^+	512(b)	524(a_g)	519(e)	569(b_1)	ν_{23}^-	511(a)	523(a_u)	519(e)	533(a_2)
ν_{24}^+	456(a)	459(a_u)	455(e)	469(a_2)	ν_{24}^-	453(b)	455(a_g)	455(e)	466(b_1)
ν_{27}^+	565(a)	569(a_g)	563(a_2)	580(a_2)	ν_{27}^-	565(b)	567(a_u)	563(b_1)	576(a_2)
ν_{28}^+	205(a)	207(a_g)	213(b_1)	197(a_2)	ν_{28}^-	203(b)	201(a_u)	182(a_2)	189(a_2)
ν_{31}^+	473(a)	474(a_g)	472(b_2)	480(b_1)	ν_{31}^-	469(b)	469(a_u)	472(a_1)	477(a_1)
ν_{32}^+	188(a)	187(a_g)	181(a_1)	182(a_1)	ν_{32}^-	185(b)	180(a_u)	176(b_2)	180(b_1)

[a] The frequencies are scaled by the factor calculated in the monomer.

Table 5. Calculated Frequency (cm^{-1}) of the Intermolecular Vibrational Modes of the Naphthalene Dimer in the MP2/cc-pVDZ Calculation without CP[a]

a	b	c	d
22(a)	8(a_u)	2(b_1)	5(b_1)
45(b)	39(a_g)	15(e)	22(a_2)
64(a)	54(a_g)	15(e)	34(b_2)
95(b)	81(a_u)	92(e)	60(b_2)
103(a)	100(a_u)	92(e)	62(a_1)
106(a)	110(a_g)	94(a_1)	69(b_1)

[a] The frequencies are not scaled.

without CP by 0.85−0.94 kcal/mol in structures **a**−**c** and by 0.25 kcal/mol in structure **d**. The effect of the CP correction on the binding energy is more enhanced in the structures dominated by the $\pi-\pi$ interaction.

Frequencies of the Vibrational Modes of the Naphthalene Dimer. The vibrational analysis of the naphthalene dimer was performed using only the geometry optimized without the CP correction, because GAUSSIAN 03 does not provide the vibrational analysis with CP. The calculated frequencies of the vibrational modes of the naphthalene dimer are listed in Table 4 for the intramolecular vibrations and in Table 5 for the intermolecular ones. Under an assumption that the vibrational motions within the naphthalene moieties is hardly disturbed by the intermolecular interactions, the intramolecular modes of the dimer are described as a linear combination of the modes of the monomer. The assignment of the intramolecular modes is also given in Table 4. The linear combination of one mode of the monomer leads to the formation of two modes of the dimer. We denoted the modes with higher frequency as ν_j^+ and those with lower frequency as ν_j^-. A detailed assignment was avoided in the *r*(CH) type, because various modes of the monomer are mixed in the vibration of the dimer. The frequencies of the intramolecular modes are scaled by the averaged factor in the monomer (Table 2), while those of the intermolecular modes are not scaled.

Discussion

Relative Stability among Isomers of Naphthalene Dimer. As shown in Figure 2, there are four stable isomers in the MP2/cc-pVDZ optimization with the vibrational analysis, although there have been eight stable isomers in MP2/6-31G*.[20] The presence of extra structures in the MP2/6-31G* calculation is attributed to a poor description of the potential energy surface, which is evident from the nonplanar structure of the naphthalene monomer in MP2/6-31G* (Table 1). Thus, for the calculation of the naphthalene dimer we should employ 6-31G*(0.25) or Dunning's correlation consistent basis sets in the MP2 method.

The ordering of the binding energy of the naphthalene dimer is **a** > **b** > **c** > **d** in the MP2/cc-pVDZ calculation without the CP correction. The ordering is kept in the single point calculation at the MP2/aug-cc-pVDZ//MP2/cc-pVDZ level. Moreover, the CP-corrected optimization does not change the ordering in MP2/cc-pVDZ without CP. The calculated results ensure us that structure **a** is most stable among the isomers in the MP2 method. Tsuzuki et al. have estimated the binding energy of the isomers including structures **b** and **c** in the CCSD(T)/6-31G* calculation (structures **a** and **d** were neglected in their work).[21] Comparing the binding energy between CCSD(T)/6-31G* and MP2/6-31G*, they showed the overestimation of the binding energy in the MP2 calculation. However, the results of the CCSD(T) calculation suggested structure **b** is more stable than structure **c**. This ordering of the binding energy agrees with our results. Thus, we assume that the ordering of the binding energy in MP2 is maintained in CCSD(T).

The symmetry of structures **a** (C_2) and **b** (C_i) is lower than that of structure **c** (D_{2d}), while the ordering of the binding energy is **a** > **b** > **c**. It means that the $\pi-\pi$ interaction is enhanced in the structures with lower symmetry. The enhancement of the $\pi-\pi$ interaction can be explained based on a molecular-orbital model (Figure 3). To simplify our explanation, we compare only structures **a** and **c**. The same discussion is true for structure **b**. In this model, the molecular orbitals of the naphthalene dimer are formed by the interaction between the highest occupied molecular orbitals (HOMOs) of the naphthalene monomers and by that between the lowest unoccupied molecular orbitals (LUMOs). The interaction between HOMO and LUMO is neglected because they have different symmetry. Considering the overlap between the molecular orbitals of the naphthalene molecules, the molecular orbitals of structure **a** are composed of a bonding orbital between HOMOs (**A1**), an antibonding orbital between HOMOs (**A2**), a bonding orbital between LUMOs (**A3**), and an antibonding orbital between LUMOs (**A4**). The electrons are occupied in orbitals **A1** and **A2** but are unoccupied in orbitals **A3** and **A4**. The occupied orbitals in structure **a** can interact with the unoccupied ones, because the symmetry is the same between orbitals **A1** and **A3** (a symmetry) and between orbitals **A2** and **A4** (b symmetry). The interaction of the occupied orbitals with the unoccupied ones contributes to the stabilization of structure **a**. On the other hand, the molecular orbitals of structure **c** are composed of a bonding orbital between HOMOs (**C1**), an antibonding orbital between HOMOs (**C2**), and nonbonding orbitals originating from LUMOs (**C3**). The electrons are occupied in orbitals **C1** and **C2** but are unoccupied in orbitals **C3**. In structure **c**, the occupied orbitals (b_1 and a_2 symmetry) do not interact with the unoccupied ones (e symmetry), because the symmetry of the orbitals is different between orbitals **C1** and **C3** and between orbitals **C2** and **C3**. Thus, structure **c** is not stabilized by the interaction between the occupied and unoccupied orbitals. Based on the above discussion, we conclude that the lowering of the symmetry enables the occupied orbitals to interact with the unoccupied ones.

Comparison of the Infrared Spectrum among the Isomers. As shown in Figure 2, the naphthalene dimer has four stable isomers. Experimentally, the isomers are distinguished based on the observed vibrational spectrum. For this purpose, we have investigated the difference of the calculated vibrational spectrum among the isomers. Table 4 suggests that the difference of the frequency is most evident in the τ(CCC)-type modes. Figure 4 shows the calculated infrared spectrum of structures **a**−**d** in the region of 150−600 cm^{-1}, where the vibrational bands of the τ(CCC) and α(CCC) type

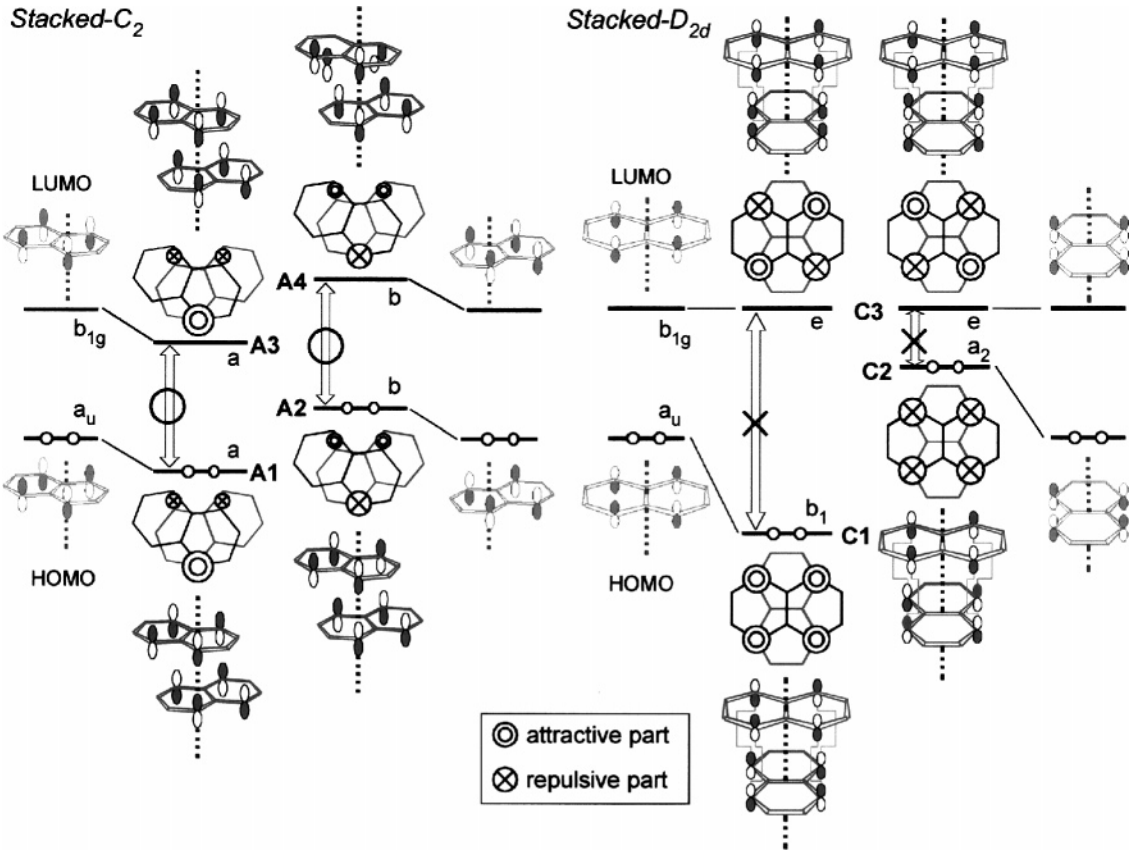

Figure 3. Schematic diagram of molecular-orbital interactions in structures **a** and **c**. The orbitals of the naphthalene dimer are formed by the interaction between HOMOs and by that between LUMOs. The orbitals with the same phase form the attractive part, while those with different phases form the repulsive one. Considering the condition of the overlap between molecular orbitals, we attributed **A1**, **A3**, and **C1** to bonding orbitals, **A2**, **A4**, and **C2** to antibonding orbitals, and **C3** to nonbonding orbitals.

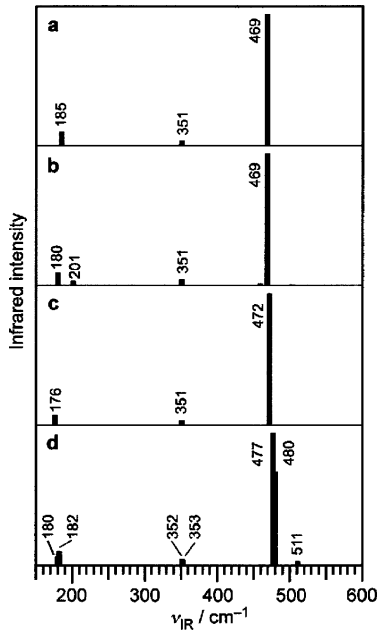

Figure 4. Calculated infrared spectrum of structures **a**−**d** in the low-frequency region. The bands around 180, 200, and 470 cm^{-1} are assigned to the τ(CCC) type, while those around 350 and 510 cm^{-1} are assigned to the α(CCC) one.

are observed. The most intense band is located around 470 cm^{-1} and is assigned to the $\nu_{31}^{\pm}$ mode. The band is degenerated in structures **a**−**c** and is split in structure **d**. In addition, the frequency of the band in structure **c** is blue-shifted from that in structures **a** and **b**. Structures **a** and **b** are distinguishable from the bands around 201 cm^{-1}, which are assigned to the ν_{28}^{-} mode. The band is observed in structure **b** and is absent in structure **a**. We can distinguish the isomers of the naphthalene dimer by the infrared spectrum in the low-frequency region.

Table 5 suggested that the frequencies of the intermolecular modes are below 110 cm^{-1} and largely depend on the isomers. The calculated infrared intensities, however, are <1% of the intensity of the $\nu_{31}^{\pm}$ mode (not shown). The vibrational bands of the intermolecular modes are difficult to observe in the infrared spectrum. We assume that the intermolecular modes are observable in the vibronic spectrum of the ground state.

Conclusions

We investigated the structures of the naphthalene monomer and dimer while performing a vibrational analysis. The MP2 optimization showed the naphthalene monomer has the nonplanar geometry in the 6-31G, 6-31G*, 6-31+G*, and 6-311G basis sets, while it has the planar geometry in the 6-31G*(0.25) and Dunning's correlation consistent basis sets. Based on the result of the monomer, we employed the MP2/cc-pVDZ level for calculation of the naphthalene dimer. The MP2/cc-pVDZ optimization showed the presence of structures **a**−**d** in Figure 2, which were part of the stable structures in the MP2/6-31G* calculation. The presence of

extra structures in the MP2/6-31G* calculation is attributed to a poor description of the potential energy surface, which is evident from the nonplanar structure of the monomer in MP2/6-31G*. The calculation of the naphthalene dimer should be performed using the 6-31G*(0.25) or Dunning's correlation consistent basis sets in the MP2 method.

The ordering of the binding energy is **a** > **b** > **c** > **d** in the MP2/cc-pVDZ optimization without the CP correction. The relative stability among the isomers was maintained in both the single-point calculation at the MP2/aug-cc-pVDZ//MP2/cc-pVDZ level and the CP-corrected optimization at the MP2/cc-pVDZ level. Thus, we concluded that structure **a** is most stable among the isomers. Structure **a** has lower symmetry than structure **c**. It indicates that the $\pi-\pi$ interaction is enhanced by lowering the symmetry. A discussion based on the molecular-orbital model elucidated that in the naphthalene dimer the symmetry lowering enhances the interaction between the occupied and unoccupied orbitals.

The intramolecular vibrations of the naphthalene dimer were assigned as a linear combination of the vibrational modes of the naphthalene monomer. Based on the results of the vibrational analysis, we concluded that the isomers are experimentally distinguishable from the infrared spectrum in the low-frequency region (150−600 cm^{-1}).

Acknowledgment. We would like to thank Dr. O. Dopfer for his comments about the ab initio MO calculation of the $\pi-\pi$ interaction. We are also thankful to Dr. A. Yokoyama for valuable discussions.

References

(1) Gonzalez, C.; Lim, E. C. *J. Phys. Chem. A* **2000**, *104*, 2953.

(2) Tsuzuki, S.; Uchimaru, T.; Matsumura, K.; Mikami, M.; Tanabe, K. *Chem. Phys. Lett.* **2000**, *319*, 547.

(3) Sato, T.; Tsuneda, T.; Hirao, K. *J. Chem. Phys.* **2005**, *123*, 104307.

(4) Hopkins, J. B.; Powers, D. E.; Smally, R. E. *J. Phys. Chem.* **1981**, *85*, 3739.

(5) Steed, J. M.; Dixton, T. A.; Klemperer, W. *J. Chem. Phys.* **1979**, *70*, 4940.

(6) Hobza, P.; Selzle, H. L.; Schlag, E. W. *J. Chem. Phys.* **1990**, *93*, 5893.

(7) Schauer, M.; Bernstein, E. R. *J. Chem. Phys.* **1985**, *82*, 3722.

(8) Henson, B. F.; Hartland, G. V.; Venturo, V. A.; Herts, R. A.; Felker, P. M. *Chem. Phys. Lett.* **1991**, *176*, 91.

(9) Henson, B. F.; Hartland, G. V.; Venturo, V. A.; Felker, P. M. *J. Chem. Phys.* **1992**, *97*, 2189.

(10) Venturo, V. A.; Felker, P. M. *J. Chem. Phys.* **1993**, *99*, 748.

(11) Schaeffer, M. W.; Maxton, P. M.; Felker, P. M. *Chem. Phys. Lett.* **1994**, *224*, 544.

(12) Ebata, T.; Ishikawa, S.; Ito, M.; Hyodo, S. *Laser Chem.* **1994**, *14*, 85.

(13) Engkvist, O.; Hobza, P.; Selzle, H. L.; Schlag, E. W. *J. Chem. Phys.* **1999**, *110*, 5758.

(14) Špirko, V.; Engkvist, O.; Soldán, P.; Selzle, H. L.; Schlag, E. W.; Hobza, P. *J. Chem. Phys.* **1999**, *111*, 572.

(15) Saigusa, H.; Sun, S.; Lim, E. C. *J. Phys. Chem.* **1992**, *96*, 2083.

(16) Saigusa, H.; Lim, E. C. *Acc. Chem. Res.* **1996**, *29*, 171.

(17) East, A. L. L.; Lim, E. C. *J. Chem. Phys.* **2000**, *113*, 8981.

(18) Song, J. K.; Han, S. Y.; Chu, I.; Kim, J. H.; Kim, S. K.; Lyapustina, S. A.; Xu, S.; Nilles, J. M.; Bowen, K. H., Jr. *J. Chem. Phys.* **2002**, *116*, 4477.

(19) Lee, N. K.; Park, S.; Kim, S. K. *J. Chem. Phys.* **2002**, *116*, 7902. Lee, N. K.; Park, S.; Kim, S. K. *J. Chem. Phys.* **2002**, *116*, 7910.

(20) Walsh, T. R. *Chem. Phys. Lett.* **2002**, *363*, 45.

(21) Tsuzuki, S.; Honda, K.; Uchimaru, T.; Mikami, M. *J. Chem. Phys.* **2004**, *120*, 647.

(22) Gonzalez, C.; Lim, E. C. *Chem. Phys. Lett.* **2000**, *322*, 382.

(23) Piuzzi, F.; Dimicoli, I.; Mons, M.; Millié, P.; Brennerm, V.; Zhao, Q.; Soep, B.; Tramer, A. *Chem. Phys.* **2002**, *275*, 123.

(24) Frisch, M. J.; et al. *Gaussian 98, revision A.11*; Gaussian, Inc.: Pittsburgh, PA, 1998.

(25) Frisch, M. J.; et al. *Gaussian 03, revision C.01*; Gaussian, Inc.: Wallingford CT, 2004.

(26) Šponer, J.; Leszczynski, J.; Hobza, P. *J. Mol. Struct.: Theochem* **2001**, *573*, 43.

(27) Boys, S. F.; Bernardi, F. *Mol. Phys.* **1970**, *19*, 553.

(28) Simon, S.; Duran, M.; Dannenberg, J. J. *J. Chem. Phys.* **1996**, *105*, 11024.

(29) Kroon-Batenburg, L. M. J.; Van Duijneveldt, F. B. *J. Mol. Struct.: Theochem* **1985**, *121*, 185.

(30) Bastiansen, O.; Skancke, P. N. *Adv. Chem. Phys.* **1961**, *3*, 323.

(31) Pauzat, F.; Talbi, D.; Miller, M. D.; DeFrees, D. J.; Ellinger, Y. *J. Phys. Chem.* **1992**, *96*, 7882.

(32) Krainov, E. P. *Opt. Spektrosk.* **1964**, *16*, 415 and 763.

(33) Martin, J. M. L.; Taylor, P. R.; Lee, T. J. *Chem. Phys. Lett.* **1997**, *275*, 414.

(34) Yagi, K.; Hirao, K.; Taketsugu, T.; Schmidt, M. W.; Gordon, M. S. *J. Chem. Phys.* **2004**, *121*, 1383.

CT050278N